

## Aromatic Expanded Isophlorins: Stable $30\pi$ Annulene Analogues with Diverse Structural Features

J. Sreedhar Reddy<sup>†</sup> and Venkataramanarao G. Anand<sup>†,\*</sup>

Chemical Sciences & Technology Division, National Institute for Interdisciplinary Science and Technology, Trivandrum 695019, India, and Department of Chemistry, Indian Institute of Science Education and Research, Sai Trinity Building, Garware Circle, Sutarwadi, Pashan, Pune 411021, India

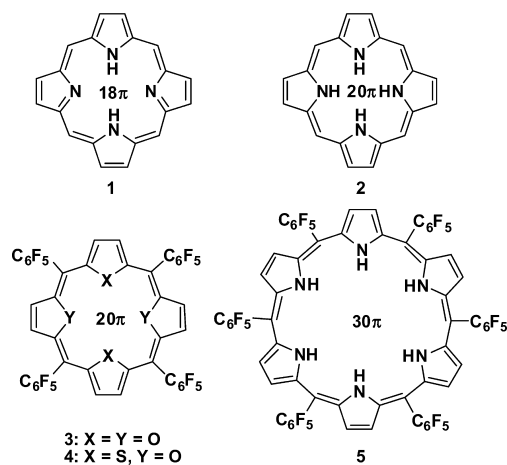
Received July 27, 2009; E-mail: vg.anand@iiserpune.ac.in

**Abstract:** Synthesis and structural diversity of novel aromatic expanded isophlorins are described. Expanded isophlorins are higher analogues of  $20\pi$  isophlorin;  $30\pi$  isophlorins are the simplest examples of expanded isophlorins. They are synthesized from easy to make precursors. Owing to the  $sp^2$  carbons along the conjugated network, they represent higher analogues of annulenes which are not realized until date. In contrast to the parent isophlorin **2**, expanded isophlorins **7–9** and **11–13** are aromatic  $(4n + 2)\pi$  systems and also differ in their optical properties and structural features. They exhibit ring inverted structures and the number of ring inversions is dependent on the nature of the heteroatoms present in the core of the macrocycle. This was confirmed by both  $^1\text{H}$  NMR spectroscopy and single crystal-ray diffraction analysis. The upfield chemical shifts for the protons of the inverted rings confirmed the diatropic ring current effects as expected for  $(4n + 2)\pi$  aromatic systems. Solid state analysis revealed a planar conformation for **7** and near planar conformations for other macrocycles. They also show strong intermolecular interactions through  $\text{C}(sp^2)\text{--H}\cdots\text{F}\text{--C}(sp^2)$  hydrogen bonds.

### Introduction

Naturally occurring conjugated macrocycles such as porphyrin, **1**, and corrin have enthused chemists to synthesize similar structural motifs with tunable electronic properties.<sup>1</sup> Isophlorin, **2**, is one such macrocycle that retains the conjugated network, but can differ in its electronic property owing to the  $20\pi$  antiaromatic nature.<sup>2,3</sup> Isophlorin's inherent unstable nature, due to rapid conversion to porphyrin, has eluded its isolation and characterization under ambient conditions. Chen et al. reported that  $\beta$ -substituted electron withdrawing trifluoromethyl groups on the pyrrole could form relatively air stable  $20\pi$  porphyrin, with resemblance to isophlorin.<sup>4</sup> Similar air sensitive  $20\pi$  porphyrin complexes of B, Si, and Ge have been derived from their corresponding porphyrin complexes, respectively.<sup>5–7</sup> Recently, we reported that the electron deficient pentafluorophenyl substituents on *meso* carbons yield air-stable  $20\pi$  isophlorins,

**Chart 1.**  $18\pi$  Porphyrin,  $20\pi$  Isophlorin, and  $30\pi$  Expanded Isophlorin



**3** and **4**.<sup>8</sup> These planar and antiaromatic isophlorin derivatives of furan and thiophene have opened new vistas for conjugated macrocyclic chemistry (Chart 1).

The structures of **3** and **4** were found to depend on the heteroatoms present in the core of the macrocycle. The tetraoxaisophlorin, **3**, is a flat square, while **4** becomes a flat rectangle even though both have a formal count of  $20\pi$  electrons. This is attributed to the two bulky sulfur atoms at the center, which occupy more space thereby pushing the two oxygen atoms away from the center. In comparison to **3**, the chemical shifts

(8) Reddy, J. S.; Anand, V. G. *J. Am. Chem. Soc.* **2008**, *130*, 3718–3719.

<sup>†</sup> NIIST, Trivandrum.

<sup>‡</sup> IISER, Pune.

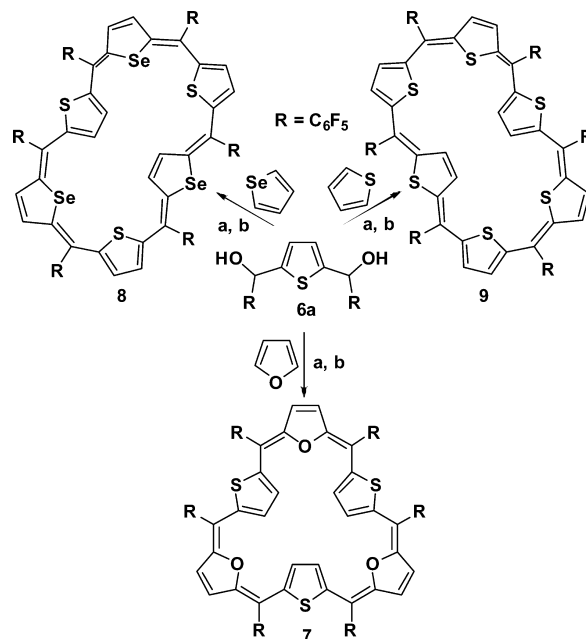
- (1) *The Porphyrin Handbook*; Kadish, K. M.; Smith, K. M.; Guillard, R., Eds.; Academic Press: New York, 2000.
- (2) (a) Woodward, R. B. *Angew. Chem.* **1960**, *72*, 651–662. (b) Woodward, R. B. *Ind. Chem. Belg.* **1962**, *27*, 1293–1308.
- (3) Vogel, E.; Gescheidt, G.; Gerson, F.; Bechmann, R. *J. Am. Chem. Soc.* **1992**, *114*, 10855–10860.
- (4) Liu, C.; Shen, D.-M.; Chen, Q.-Y. *J. Am. Chem. Soc.* **2007**, *129*, 5814–5815.
- (5) Weiss, A.; Hodgson, M. C.; Boyd, W. P. D.; Siebert, W.; Brothers, P. J. *J. Chem.—Eur. J.* **2007**, *13*, 5982–5993.
- (6) Ciessell, J. A.; Vaid, T. P.; Rheingold, A. L. *J. Am. Chem. Soc.* **2005**, *127*, 12212–12213.
- (7) Ciessell, J. A.; Vaid, T. P.; Yap, G. P. A. *J. Am. Chem. Soc.* **2007**, *129*, 7841–7847.

of the furan protons were downfield shifted for **4** indicating the dependence of ring current effects on the structure of the macrocycle. Structural modification of similar macrocycles has surfaced in phospha-thiaporphyrin, which undergoes redox coupled complexation with metals such as Ni, Pd and Pt to yield isophlorin like macrocycle, highlighting the structure induced effects on optical and electronic properties.<sup>9</sup> Design and synthesis of cyclic assemblies using small aromatic units with varying constitution or size have become attractive targets for tuning optical and electronic properties of organic materials.<sup>10,11</sup> Varying the extent of the  $\pi$ -conjugated network of isophlorins is an alternative strategy to significantly alter its electronic properties. The length of the  $\pi$  network increased by inserting additional heterocyclic rings in modified isophlorins like **3** and **4**, will lead to a new class of macrocycles which we wish to term as *expanded isophlorins*. Structurally, expanded isophlorins are higher homologues of isophlorin which form  $10n\pi$  systems when a ratio of 1:1 is sustained between the number of heterocyclic subunits and the bridging *meso* carbons. The simplest expanded isophlorin consists of six heterocyclic rings, since an odd number of heterocyclic rings with an equal number of bridging carbons fails to attain isophlorin-type cyclic conjugation. For all odd integral values of  $n$ ,  $10n\pi$  systems will satisfy  $(4n + 2)\pi$  Huckel rule, whereas, even integral values of  $n$  should conceive antiaromatic  $10n\pi$  systems. For example, six pyrrole units when connected in a cyclic fashion should form **5**, a  $30\pi$ -expanded isophlorin. Since such a macrocycle has not been realized until date, it can be considered as an intermediate during the formation of  $26\pi$ - or  $28\pi$ -expanded porphyrins.<sup>12</sup> Macrocylic oligofurans with six and eight furan units resemble expanded isophlorins generated by insertion of additional heterocyclic units.<sup>13</sup> Insight into ring current effects in such archetype structures has been obscured by lack of apt synthetic routes. Herein, we wish to report the synthesis and structural diversity of aromatic  $30\pi$  expanded isophlorins, in which all the nitrogens (as in **5**) are replaced by chalcogens such as oxygen, sulfur, and selenium.

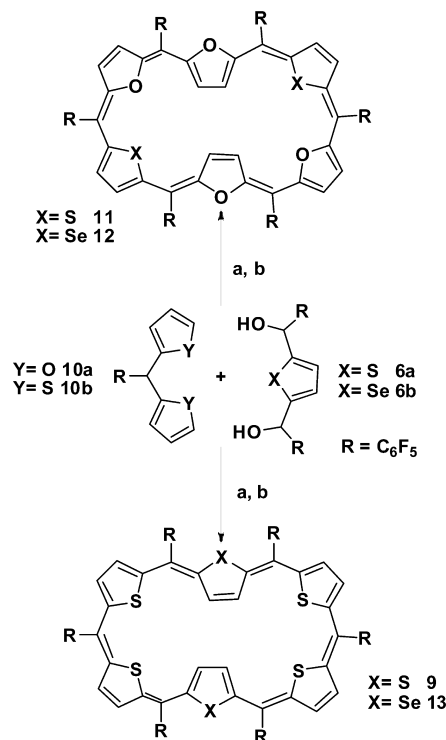
## Results and Discussion

**Synthesis.** Depending on the nature of the precursors, two different synthetic routes (Schemes 1 and 2), were employed to synthesize the expanded isophlorins. In a simple procedure (Scheme 1),  $\text{BF}_3 \cdot \text{OEt}_2$  catalyzed condensation of 2,5-(pentafluorophenylhydroxymethyl)thiophene, **6a**,<sup>14</sup> with different heterocycles furan, thiophene, and selenophene yielded three different  $30\pi$ -expanded isophlorins; 5,10,15,20,25,30-hexa(pentafluoro)phenyl-31,33,35-trioxa-32,34,36-trithiaisophlorin, **7**, 5,10,15,20,25,30-hexa(pentafluoro)phenyl-31,33,35-triselenaisophlorin, **8**, and 5,10,15,20,25,30-hexa(pentafluoro)phenyl-31,33,35-trithiaisophlorin, **9**. Similar reactions with either furan diol or selenophene diol were not equally successful. The pentafluorophenyl derivative of furan diol was found to be unstable and hence could not be utilized in condensation reactions. Selenophene diol, **6b**,<sup>14</sup> when reacted with other heterocycles under similar conditions yielded a variety of conjugated macrocycles, whose details will be published elsewhere. In an alternative procedure (Scheme 2), both 2,2'-(pentafluorophenylmethylene)difuran, **10a**,<sup>14</sup> and 2,2'-(pentafluorophenylmethylene)dithiophene, **10b**,<sup>14</sup> were used as precursors. Reaction of **10a** with thiophene or selenophene yielded 32,34,36-trithiaisophlorin, **11**, and 32,34,36-triselenaisophlorin, **12**, respectively. Reaction of **10b** with thiophene or selenophene yielded 32,34,36-trithiaisophlorin, **13**, and 32,34,36-triselenaisophlorin, **14**, respectively.

**Scheme 1.** Synthesis of **7–9**: (a) 0.5 equiv  $\text{BF}_3 \cdot \text{OEt}_2$ ,  $\text{CH}_2\text{Cl}_2$ , 2 h; (b) 2.5 equiv  $\text{FeCl}_3$ , 2 h.



**Scheme 2.** Synthesis of **11–13**: (a) 0.5 equiv  $\text{BF}_3 \cdot \text{OEt}_2$ ,  $\text{CH}_2\text{Cl}_2$ , 2 h; (b) 2.5 equiv  $\text{FeCl}_3$ , 2 h.



32,34,36-trithiaisophlorin, **8**, and 5,10,15,20,25,30-hexa(pentafluoro)phenyl-31,32,33,34,35,36-hexathiaisophlorin **9**. Similar reactions with either furan diol or selenophene diol were not equally successful. The pentafluorophenyl derivative of furan diol was found to be unstable and hence could not be utilized in condensation reactions. Selenophene diol, **6b**,<sup>14</sup> when reacted with other heterocycles under similar conditions yielded a variety of conjugated macrocycles, whose details will be published elsewhere. In an alternative procedure (Scheme 2), both 2,2'-(pentafluorophenylmethylene)difuran, **10a**,<sup>14</sup> and 2,2'-(pentafluorophenylmethylene)dithiophene, **10b**,<sup>14</sup> were used as precursors. Reaction of **10a** with thiophene or selenophene yielded 32,34,36-trithiaisophlorin, **11**, and 32,34,36-triselenaisophlorin, **12**, respectively. Reaction of **10b** with thiophene or selenophene yielded 32,34,36-trithiaisophlorin, **13**, and 32,34,36-triselenaisophlorin, **14**, respectively.

- (9) Matano, Y.; Nakabuchi, T.; Fujishige, S.; Nakano, H.; Imahori, H. *J. Am. Chem. Soc.* **2008**, *130*, 16446–16447.
- (10) (a) Kromer, J.; Rios-Carreras, I.; Fuuhrmann, G.; Musch, C.; Wunderlin, M.; Debaerdemaeker, T.; Mena-Osteritz, E.; Bauerle, P. *Angew. Chem., Int. Ed.* **2000**, *39*, 3481–3484. (b) Nakao, K.; Nishimura, M.; Tamachi, T.; Kuwatani, Y.; Miyasaka, H.; Nishinaga, T.; Iyoda, M. *J. Am. Chem. Soc.* **2006**, *128*, 16740–16747.
- (11) Torroba, T.; Valverde, M. G. *Angew. Chem., Int. Ed.* **2006**, *45*, 8092–8096.
- (12) (a) Neves, M. G. P. M. S.; Martins, R. M.; Tome, A. C.; Silvestre, J. D.; Silva, A. M. S.; Felix, V.; Drew, M. G. B.; Cavalerio, J. A. S. *Chem. Commun.* **1999**, 385–386. (b) Shimizu, S.; Shin, J. Y.; Furuta, H.; Ismael, R.; Osuka, A. *Angew. Chem., Int. Ed.* **2003**, *42*, 78–82.
- (13) Reddy, J. S.; Mandal, S.; Anand, V. G. *Org. Lett.* **2006**, *8*, 5541–5543.
- (14) Lee, C. H.; Kim, H. J.; Yoon, D. W. *Bull. Korean Chem. Soc.* **1999**, *20*, 276–280.

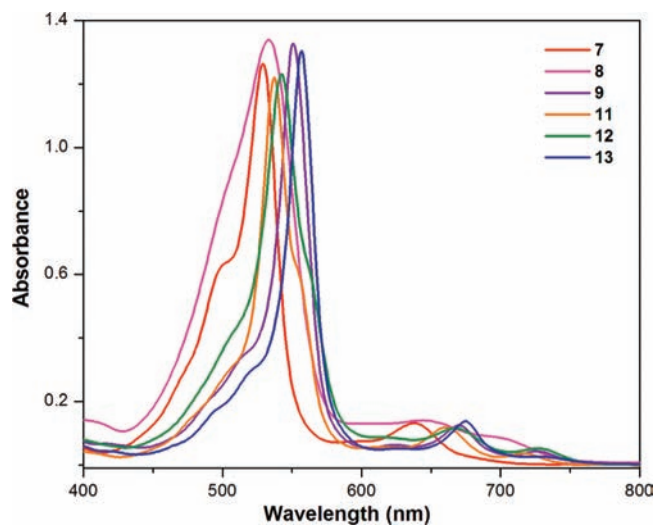


**Figure 1.** Electronic absorption spectrum of  $10^{-6}$  M solutions of **7–9** and **11–13** in  $\text{CH}_2\text{Cl}_2$ .

tafluorophenylmethylene)dithiophene, **10b**,<sup>14</sup> were condensed with diols **6a** and **6b**, under identical conditions as mentioned above, to yield three different expanded isophlorins; 5,10,15,20,25,30-hexa(pentafluoro)phenyl-31,32,34,35-tetraoxa-33,36-dithiaisophlorin, **11**, 5,10,15,20,25,30-hexa(pentafluoro)phenyl-31,32,34,35-tetraoxa-33,36-diselenaisophlorin, **12**, and 5,10,15,20,25,30-hexa(pentafluoro)phenyl-31,34-diselena-32,33,35,36-tetrathiaisophlorin, **13** (Schemes 1 and 2). It is pertinent to note that an earlier attempt could not accomplish the synthesis of **9** from methylene-bridged cyclohexathiophene,<sup>15</sup> while another report of 30 $\pi$  heteroazaporphyrinoid<sup>16</sup> turned out to be nonaromatic in spite of its delocalized  $\pi$  electrons.

**Characterization.** All the macrocycles mentioned above were characterized by various analytical techniques and by single crystal X-ray diffraction studies, wherever possible, before arriving at their final structure. Because of extensive conjugation, all these molecules show colored solution in common organic solvents and absorb intensely in the visible region of the electromagnetic spectrum (Figure 1). Even though all the macrocycles have a  $\text{sp}^2$  carbon conjugated network, these macrocycles display substantial changes in their photophysical properties. Depending on the kind of chalcogens present in the core of the macrocycle, **7**, **8**, **9**, **11**, **12**, and **13**, show an intense absorption band ( $\epsilon = 10^4$ ) in the range 529–557 nm and low intense bands in between 638 and 726 nm. This variation can be attributed to either structural changes or unequal participation of the heteroatoms in the globalized delocalization of  $\pi$  electrons for a given macrocycle. No significant changes in their electronic absorption spectrum upon addition of oxidizing agents such as trifluoroacetic acid, DDQ, and perchloric acid suggested that these macrocycles are very stable.

Proton NMR analysis of all the macrocycles confirmed their aromatic behavior (see Supporting Information, SI).  $^1\text{H}$  NMR spectrum of **7** exhibits only two singlets at  $\delta$  7.99 and 1.87 ppm, indicative of a highly symmetrical structure. Two discrete singlets reflect two different environments for the protons of thiophene and furan rings. This can be possible only when three

furan (or thiophene) rings are inverted. The protons of the inverted rings experience the diatropic ring current effect of the 30 $\pi$  system and hence are found to resonate at high field. This is justified by the upfield shift of nearly 4 ppm for the  $\beta$ -CH protons in comparison to their chemical shift values in unsubstituted thiophene or furan. Such shifts can be envisaged only when the macrocycle adopts a flat and  $D_{3h}$  symmetry. Variable temperature  $^1\text{H}$  NMR did not show any variation in the spectrum pattern, confirming the absence of any fluxionality in solution state. The proton NMR spectrum changes drastically when the three furans are replaced by three selenophenes in the macrocycle. **8** exhibits two doublets and a multiplet in the region between  $\delta$  8.16 and 7.9 ppm corresponding to eight protons each, along with two singlets corresponding to two protons each at  $\delta$  3.79 and 3.26 ppm. The increased number of signals, with respect to **7**, signifies the reduced symmetry of the macrocycle. The upfield proton resonances can be attributed to inversion of a thiophene and selenophene ring, respectively, while the low-field resonance appears for the protons of the two noninverted thiophene and selenophene rings each. Even though thiophene and selenophene rings alternate with each other, similar to S and O as in **7**, the three bigger Se may be sterically hindered to be accommodated in the cavity of the macrocycle and hence only two ring inversions can be anticipated for the reduced symmetry of **8**. The NMR spectrum shows enhanced symmetry when all the selenophene rings in **8** are replaced by thiophene units. **9** shows three different signals corresponding to four protons each. Two doublets at  $\delta$  9.18 and 9.09 ppm corresponding to eight protons and a singlet at  $\delta$  -0.46 ppm for four protons account for all the twelve protons of **9**. The upfield singlet suggests a symmetrical inversion of thiophene rings. This is possible only if the two diagonally opposite thiophene rings are inverted and the protons of those rings experience the diatropic ring current to resonate at high field. Macrocycles **7**, **8**, and **9** have three thiophene rings in common among themselves, but dissimilar ring inversions in the macrocycles alter their structural features. **11** and **12** have four oxygen atoms along with two S and two Se atoms, respectively. They exhibit similar  $^1\text{H}$  NMR spectrum, bearing six doublets corresponding to twelve protons. Four doublets resonate at  $\delta$  9.07, 8.92, 8.63, and 8.58 ppm, while two more doublets resonate at  $\delta$  -0.17 and -0.7 ppm for **11**. The absence of singlets suggests a lower symmetry arising from unsymmetrical ring inversions. A similar spectrum, with four doublets at  $\delta$  9.04, 8.93, 8.45, and 8.4 ppm, along with two doublets at  $\delta$  0.88 and 0.41 ppm were observed for **12**, suggesting a similar structure as of **11**. As observed for **8** and **9**, we expected symmetrical ring inversions of two thiophenes in **11** and two selenophenes in **12**. Absence of a singlet in  $^1\text{H}$  NMR spectrum, for the inverted ring protons in **11** and **12**, ascertains that two diagonally opposite furans undergo inversion in both **11** and **12**, leading to the doublets in the upfield region. The  $^1\text{H}$  NMR spectrum of **13**, with four sulfurs and two selenium atoms, was found to be similar with that of hexathiophene macrocycle **9**. Two doublets at  $\delta$  9.23 and 9.14 ppm corresponding to eight protons and a singlet at -0.87 ppm for four protons were observed, suggestive of symmetrical ring inversions from the two diagonally opposite selenophene rings. The upfield resonance for the protons of the inverted heterocyclic rings indicates the diatropic ring current effect due to its aromatic character. The  $\Delta\delta$  (difference in the ppm value between most shielded and deshielded protons) values calculated (Table 1) as a measure of aromaticity vary

(15) Sessler, J. L.; Gebauer, A.; Weghorn, S. J. In *The Porphyrin Handbook*; Kadish, K. M.; Smith, K. M.; Guillard, R., Eds.; Academic Press: New York, 2000; Vol. 2, 93.

(16) Islyaikin, M. K.; Danilova, E. A.; Yagodarova, L. D.; Rodriguez-Morgade, M. S.; Torres, T. *Org. Lett.* **2001**, 3, 2153–2156.



Table 1.  $\Delta\delta$  Values

macrocycle	$\Delta\delta$
7	6.12
8	4.9
9	9.63
11	9.77
12	8.63
13	10.1

from 4.9 to 10.1, implying the aromatic nature of all the macrocycles described above.

**Single Crystal X-ray Diffraction Analysis.** The single crystal X-ray diffraction analysis confirmed the structures of **7**, **8**, **9**, **11**, and **13** as analyzed through solution state studies. Good quality single crystals were obtained for all the macrocycles except for **12**. The crystal structure of **7** confirmed the inversion of three thiophene rings. It crystallizes in orthorhombic system with space group *Pmnm*. One-fourth of the molecule forms the asymmetric unit. There are two molecules in the unit cell (see SI). The crystallographic mirror plane normal to *b*-axis (at one-fourth of *b*) coincides with the molecular plane. This makes the molecular plane, defined by the six *meso* carbons, ideally flat in nature (Figure 2a). The planarity of **7** can also be attributed to the symmetrical inversion of three thiophene rings, which probably reduces the steric strain on the molecule. The *meso* pentafluorophenyl rings are exactly perpendicular to molecular plane with a 90° angle. The three oxygens O–O–O (or sulfurs) form an angle of 60°, and hence the shape resembles that of an equilateral triangle. Multiple ring inversions with a triangular shape have been observed recently for 26 $\pi$ -aromatic macrocycles,<sup>17</sup> but this is the first report for a 30 $\pi$ -aromatic system. Further analysis revealed the intermolecular interactions in the crystal lattice. The  $\beta$ -hydrogen ( $H_3$ ) of the asymmetric unit forms two symmetrically equivalent hydrogen bonds (i.e., bifurcated hydrogen bond) with F8 and its mirror equivalent. The symmetries of F8 are  $1-x, 1-y, 2-z$ , and  $1-x, 1/2+y-1, 2-z$ . Thus there are four intermolecular C–H $\cdots$ F hydrogen bonds (2.71 Å, 143°) with four neighboring molecules linking through hydrogen ( $H_3$ ) atoms. In addition to these four, the four F8 atoms of a given molecule become acceptors for four more hydrogen bonds. Therefore, there are eight hydrogen-bonded links from a given molecule to its neighborhood, to form a three-dimensional hydrogen-bonded network in the crystal lattice<sup>18,19</sup> (Figure 3).

The solid state analysis of **8**, which crystallized with space group *P1*, revealed a rectangular-shaped macrocycle with two diagonally inverted heterocyclic rings which contain sulfur and selenium as heteroatoms (Figure 2b). The inverted thiophene and the selenophene rings are tilted above and below the mean plane leading to nonplanar conformation. They deviate by 15.02° and 16.3° from the mean macrocyclic plane defined by six *meso* carbons. The symmetry of the macrocycle makes it difficult to exactly distinguish between S and Se, and hence the sulfur and selenium positions could not be precisely determined in solid

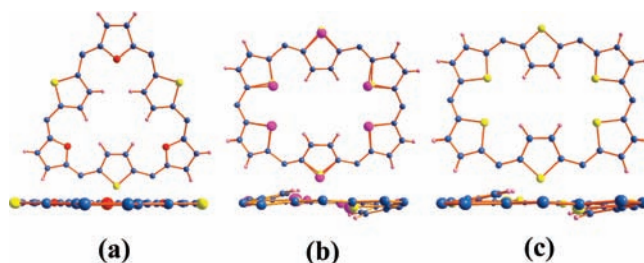


**Figure 2.** Single crystal X-ray structures. Top view (above) and side view (below) of **7** (a), **8** (b), and **9** (c). *Meso* pentafluorophenyl rings and solvent molecules are deleted for clarity. Hydrogen atoms of inverted rings alone are shown in the side view. Color code: carbon (blue), hydrogen (pink), oxygen (red), selenium (magenta), and sulfur (yellow). The same code is followed for other crystal structure images.

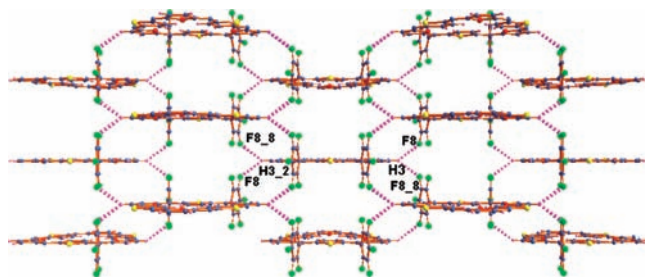


**Figure 3.** Hydrogen bonding interactions observed in crystal packing of **7**. Only pentafluorophenyl rings of the fluorines involved in hydrogen bonding are shown for clarity.

state. The distance between neighboring hetero atoms (Se and S) of noninverted rings was found to be 3.0 Å, while it is 7.0 Å between the two heteroatoms adjacent to an inverted ring. Thus, the cavity size at the center is spacious enough to accommodate four  $\beta$  C–H's from two different heterocyclic rings.

The crystal structure of hexathiaisophlorin, **9**, also exposed a rectangular-shaped macrocycle with two diagonally inverted thiophene rings (Figure 2c). The distance between neighboring sulfur atoms of noninverted thiophene rings was found to be 2.3 Å, while it is 7.2 Å between the two sulfur atoms adjacent to an inverted thiophene ring. The inverted thiophenes were found to deviate by 12.2°, one each above and below, from the mean macrocyclic plane defined by six *meso* carbons. The crystal packing shows three different C–H $\cdots$ F interactions for each molecule of **9**. The protons of the ring inverted thiophenes form two pairs of similar hydrogen bonds [C7–H7 $\cdots$ F12 (2.81 Å, 148°; symm;  $-x, 1-y, 1-z$ ), C8–H8 $\cdots$ F11 (2.48 Å, 134°; symm;  $-x, 1-y, 1-z$ )] with fluorines of the *meso* pentafluorophenyl rings from two different molecules in head-to-tail manner leading to a one-dimensional sheetlike structure.<sup>18,19</sup> The third hydrogen bond [C12–H12 $\cdots$ F7 (2.48 Å, 145°; symm;  $1+x, y, 1+z$ )] involving a proton of the noninverted thiophene ring and a fluorine from the pentafluorophenyl ring interconnects both sheets leading to a two-dimensional supramolecular architecture (see SI). Apart from these hydrogen bonds, two different F $\cdots$ F nonbonded interactions<sup>20</sup> F1 $\cdots$ F7 (2.81 Å) and F15 $\cdots$ F15 (2.70 Å), with bond lengths less than the sum of their van der Waals radii (2.94 Å) could be observed in the crystal lattice (see SI).

Macrocycle **11** crystallized in monoclinic system with space group *P21/n*. There are four molecules in the unit cell. The solid

(17) Xie, Y. H.; Yamaguchi, K.; Toganoh, M.; Uno, H.; Suzuki, M.; Mori, S.; Saito, S.; Osuka, A.; Furuta, H. *Angew. Chem., Int. Ed.* **2009**, *48*, 5496–5499.

(18) Thalladi, V. R.; Weiss, H. C.; Blaser, D.; Boese, R.; Nangia, A.; Desiraju, G. R. *J. Am. Chem. Soc.* **1998**, *120*, 8702–8710.

(19) Desiraju, G. R.; Steiner, T. *The Weak Hydrogen Bond in Structural Chemistry and Biology*; Oxford University Press: Oxford, 1999; Chapter 3.

(20) Ramasubbu, N.; Parthasarathy, R.; Murray-Rust, P. *J. Am. Chem. Soc.* **1986**, *108*, 4308–4314.

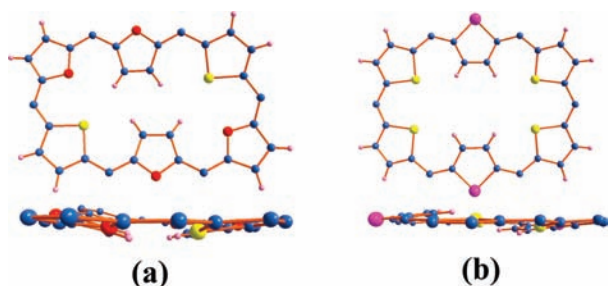


**Figure 4.** Single crystal X-ray structures. Top view (above) and side view (below) of **11** (a) and **13** (b). Meso pentafluorophenyl rings and solvent molecules are deleted for clarity. The hydrogen atoms of inverted rings alone are shown in the side view. Color code: carbon (blue), hydrogen (pink), oxygen (red), selenium (magenta), and sulfur (yellow).

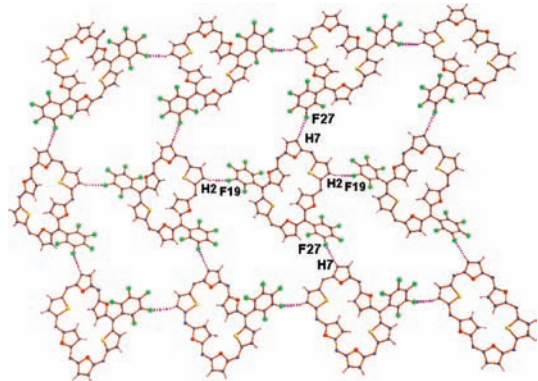


**Figure 5.** 2D gridlike supramolecular structure formed through C–H $\cdots$ F–C noncovalent interactions in crystal packing of **11**. Only pentafluorophenyl rings of the fluorines involved in hydrogen bonding are shown for clarity.

state analysis revealed a compressed rectangular-shaped macrocycle with two diagonally inverted furan rings (Figure 4a). Interestingly, both inverted furan rings are tilted in the same direction from the mean macrocyclic plane defined by six *meso* carbons. They deviated by 13.18° and 12.87°, and hence induced a bowl-shaped structure to the macrocycle. The distance between neighboring heteroatoms (S and O) of noninverted rings was found to be 2.89 and 2.91 Å, while it is 7.39 Å between the two heteroatoms (S and O) adjacent to an inverted ring. Of particular interest is the intermolecular hydrogen bonding in **11**, wherein each macrocycle has two acceptor and two donor sites for hydrogen bonding. The *meta*-fluorine from two *meso* pentafluorophenyl rings and two  $\beta$ -hydrogen atoms, one each from thiophene and furan, are involved in C–H $\cdots$ F–C interactions. Therefore each molecule forms two pairs of similar hydrogen bonds [C7–H7 $\cdots$ F27 (2.48 Å, 172°; symm; 0.5 –  $x$ , 0.5 +  $y$ , –0.5 –  $z$ ) and C2–H2 $\cdots$ F19 (2.62 Å, 159°; symm; 0.5 –  $x$ , 0.5 +  $y$ , –0.5 –  $z$ )] with four other neighbors in the same molecular plane leading to a well-defined assembly of a two-dimensional grid<sup>18,19</sup> (Figure 5). Furthermore, in crystal packing, F $\cdots$ F interactions<sup>20</sup> (F1 $\cdots$ F15) were also observed, probably aiding the crystal packing along with hydrogen bonds (see SI).

Macrocycle **13** crystallized in triclinic system in space group  $P\bar{1}$ . Its solid state analysis revealed a rectangular-shaped macrocycle with two diagonally inverted selenophene rings (Figure 4b). The inverted selenophene rings are tilted above and below the mean macrocyclic plane defined by six *meso* carbons. This makes **13** lose absolute planar conformation, since the heterocyclic rings deviate by 8.3° from the

macrocyclic plane. The distance between the neighboring two sulfur atoms of noninverted rings was found to be 2.99 Å, while it is 7.21 Å between the two sulfur atoms adjacent to an inverted ring. Similar to **9**, the crystal packing shows three different C–H $\cdots$ F–C interactions for each molecule of **13**. The protons of both the ring inverted selenophenes form two pairs of similar hydrogen bonds [C2–H2 $\cdots$ F9 (2.74 Å, 140°; symm; 2 –  $x$ , – $y$ , – $z$ ), C3–H3 $\cdots$ F10 (2.55 Å, 140°; symm; –1 +  $x$ ,  $y$ , 1 +  $z$ )] with fluorines of the *meso* pentafluorophenyl rings from two different molecules in head to tail manner leading to a one-dimensional sheetlike structure. The third hydrogen bond [C7–H7 $\cdots$ F4 (2.56 Å, 146°; symm; –1 +  $x$ ,  $y$ ,  $z$ )] involving a proton of the noninverted thiophene ring and a fluorine from the pentafluorophenyl ring interconnects both the sheets leading to a two-dimensional supramolecular architecture<sup>18,19</sup> (SI). Apart from these hydrogen bonds, F $\cdots$ F nonbonded interaction F4 $\cdots$ F15 (2.91 Å) was also detected in the crystal lattice<sup>20</sup> (SI). In all the macrocycles described above, it was observed that the C–C bond distance along the 30 $\pi$  perimeter was found to be in between single and double bond distances, confirming the delocalization of  $\pi$  electrons.

The cyclic voltammogram in all 30 $\pi$  macrocycles exhibit two oxidation and reductions (SI). The  $\Delta_{\text{redox}}$  values were calculated as the difference between the first oxidation and reduction potential obtained from DPV. The  $\Delta_{\text{redox}}$  values of **7–9** reflect the reduction in the energy gap between HOMO–LUMO (highest occupied molecular orbital–lowest unoccupied molecular orbital) as observed by the red shifts in their electronic spectra. Similar observation has been made for **11–13**, suggesting the increased contribution by the heavy atoms to the  $\pi$  conjugation in the macrocycles. The redox potentials calculated at 100 mv/s in dry CH<sub>2</sub>Cl<sub>2</sub>, with TBAPF<sub>6</sub> as supporting electrolyte, were found to be quasi-reversible. These  $\Delta_{\text{redox}}$  potentials are comparable with the earlier reported 30 $\pi$ -expanded porphyrins.<sup>21</sup> Hence it further justifies that these macrocycles have effective  $\pi$  electron delocalization and are aromatic in nature.

## Conclusions

We have described the syntheses and characterization of unprecedented aromatic 30 $\pi$  expanded isophlorins composed of furan, thiophene, and selenophene. They adopt different ring inverted structures depending on the nature of the heteroatoms present in the core of the macrocycle, which in turn is reflected in their electronic property. To the best of knowledge, hexathioisophlorin, **9**, is the first macrocyclic oligothiophene to display annulenoid-type delocalization of  $\pi$  electrons as evidenced from <sup>1</sup>H NMR spectroscopy and also from electronic absorption spectroscopy. Similar structural and electronic property is observed in the case of other macrocyclic oligoheterocyclics described above, and this is a new class of annulenoid systems exhibiting ring current effects in large macrocycles. The hydrogen-bond parameters (2.48 Å, 172°), responsible for 2D grid in **11**, reflect very strong interactions which are rarely observed for C(sp<sup>2</sup>)–H $\cdots$ F–C(sp<sup>2</sup>) bonds. It is expected that such large structures with delocalized  $\pi$  electrons combined with the ability to

(21) Anand, V. G.; Pushpan, S. K.; Venkatraman, S.; Narayanan, S. J. P.; Dey, A.; Chandrashekar, T. K.; Roy, R.; Joshi, B. S.; Deepa, S.; Narahari Sastri, G. *J. Org. Chem.* **2002**, *67*, 6309–6319.

Table 2. Crystal Data for 7–9, 11, and 13

macrocycle	7	8	9	11	13
solvent syst	CHCl <sub>3</sub> /hexane	CHCl <sub>3</sub> /hexane	CHCl <sub>3</sub> /hexane	CHCl <sub>3</sub> /hexane	CHCl <sub>3</sub> /hexane
empirical formula	C <sub>66</sub> H <sub>12</sub> F <sub>30</sub> S <sub>3</sub> O <sub>3</sub>	C <sub>66</sub> H <sub>12</sub> F <sub>30</sub> S <sub>3</sub> Se <sub>3</sub>	C <sub>66</sub> H <sub>12</sub> F <sub>30</sub> S <sub>6</sub>	C <sub>66</sub> H <sub>12</sub> F <sub>30</sub> S <sub>2</sub> O <sub>4</sub>	C <sub>66</sub> H <sub>12</sub> F <sub>30</sub> S <sub>4</sub> Se <sub>2</sub>
cryst syst	orthorhombic	triclinic	triclinic	monoclinic	triclinic
space group	<i>Pmnn</i>	<i>P1</i>	<i>P1</i>	<i>P21/n</i>	<i>P1</i>
<i>a</i>	24.7594(8) Å	9.7036(4) Å	9.4066(10) Å	11.2195(8) Å	9.7879(3) Å
<i>b</i>	7.9014(3) Å	12.8407(5) Å	13.0693(14) Å	33.928(2) Å	12.8233(4) Å
<i>c</i>	21.7277(6) Å	15.7989(6) Å	15.5194(17) Å	16.4312(11) Å	15.7687(6) Å
$\alpha$	90.00	101.927(2)	103.922(2)	90.00	102.336(2)
$\beta$	90.00	92.695(2)	90.720(2)	107.115(5)	92.709(2)
$\gamma$	90.00	94.785(2)	96.358(2)	90.00	94.913(2)
<i>V</i> , Å <sup>3</sup>	4250.7(2)	1915.17(13)	1839.0(3)	5977.6(7)	1922.0(11)
<i>Z</i>	2	1	1	4	1
<i>D</i> <sub>calcd</sub>	1.257 g/cm <sup>-3</sup>	1.895 g/cm <sup>-3</sup>	1.846 g/cm <sup>-3</sup>	1.727 g/cm <sup>-3</sup>	1.847 g/cm <sup>-3</sup>
abs coeff	0.196	2.058	0.744	0.282	1.605
<i>F</i> (000)	1600	1060	1006	3072	1042
$\theta$ for data	2.5 – 20.0	1.3 – 29.56	2.6 – 25	2.5 – 19	2.6 – 25.2
limiting	–24 ≤ <i>h</i> ≤ 20 –7 ≤ <i>k</i> ≤ 7 –20 ≤ <i>l</i> ≤ 21	–13 ≤ <i>h</i> ≤ 13 –17 ≤ <i>k</i> ≤ 17 –21 ≤ <i>l</i> ≤ 21	–11 ≤ <i>h</i> ≤ 11 –10 ≤ <i>k</i> ≤ 15 –17 ≤ <i>l</i> ≤ 18	–10 ≤ <i>h</i> ≤ 10 –31 ≤ <i>k</i> ≤ 31 –15 ≤ <i>l</i> ≤ 15	–12 ≤ <i>h</i> ≤ 12 –16 ≤ <i>k</i> ≤ 16 –19 ≤ <i>l</i> ≤ 19
reflns collected	15146	47503	9487	29593	41502
independent reflns	2320	19873	6364	4920	8140
abs correction	multiscan	multiscan	multiscan	multiscan	multiscan
GOF	1.383	1.015	0.809	1.035	1.024
R1	0.1161	0.0505	0.0544	0.0973	0.0598
R2 <sub>w</sub>	0.2816	0.1238	0.1059	0.2476	0.1631

form well-defined supramolecular architectures through strong intermolecular interactions can be better materials for organic electronics.

## Experimental Section

**General Experimental Procedures.** Common solvents used for syntheses were purified according to known procedures. Thiophene, furan, and selenophene were procured from Aldrich Chemicals; except for selenophene, all others were distilled before use. Deuterated solvents for NMR measurements were used as received. Trifluoroacetic acid (TFA) and *n*-butyllithium (15% in hexane) were procured from E. Merck, Germany, and Lancaster, U.K. Anhydrous potassium carbonate, anhydrous sodium sulfate, and anhydrous calcium chloride were obtained from Qualigens Fine Chemicals, India. Aluminum oxide (basic) and silica gel (100–200 and 230–400 mesh) were purchased from Acme Chemicals, India. *N,N,N',N'*-Tetramethyl ethylenediamine was procured from Loba Chemicals, India, and was distilled over KOH before use. 2-Bromothiophene and pentafluorobenzaldehyde were used as received from Lancaster, U.K.

Electronic spectra were recorded on a Perkin-Elmer-Lambda 20 UV–vis spectrophotometer. The data analyses were done using the UV–winlab software package. <sup>1</sup>H NMR spectra were obtained either from 300 MHz Bruker Advance DPX spectrometer or from 400 MHz Jeol machine either in CDCl<sub>3</sub> or in CD<sub>2</sub>Cl<sub>2</sub>. Chemical shifts are expressed in parts per million relative to residual CHCl<sub>3</sub>/CH<sub>2</sub>Cl<sub>2</sub>. MALDI-TOF was carried out on Voyager-De-STR (Applied Biosystems). Cyclic voltammetric studies were done on EG/G PAR model 273A polarographic analysis interfaced to computer. A three-electrode system consisting of a platinum (Pt) working electrode and a commercially available saturated calomel electrode, reference electrode, and a Pt mesh counter-electrode were used. The reference electrode was separated from the bulk of solution by a fritted glass bridge filled with the solvent/supporting electrolyte mixture.

**Synthetic procedure for 7, 8, and 9.** A solution of 2,5-(pentafluorophenylhydroxymethyl) thiophene (238 mg, 0.5 mmol), **6a**, and furan or selenophene or thiophene (0.5 mmol) in 100 mL of dry dichloromethane was placed in 250 mL flask under nitrogen. BF<sub>3</sub>·OEt<sub>2</sub> (0.03 mL, 0.25 mmol) was added under dark, and the resulting solution was stirred for 1 h. After adding FeCl<sub>3</sub> (405 mg, 2.5 mmol), the solution was opened to air and stirred for 2 h more. The reaction mixture was washed with water and passed through a

short alumina column. A pink color band eluted with 5% CH<sub>2</sub>Cl<sub>2</sub> in *n*-hexane and was repeatedly purified by silica gel column chromatography. Macrocycles **7**, **8**, and **9** were isolated in 9% (68 mg), 3% (26 mg), and 11% (71 mg) yield, respectively.

**Compound 7.** <sup>1</sup>H NMR (300 MHz, CDCl<sub>3</sub>, 298 K):  $\delta$  = 7.99 (s, 6H),  $\delta$  = 1.87 (s, 6H); UV–vis (CH<sub>2</sub>Cl<sub>2</sub>):  $\lambda_{\max}(\epsilon)$  = 529(194720), 638(19900). MALDI-TOF MS *m/z*: Calcd for C<sub>66</sub>H<sub>12</sub>F<sub>30</sub>S<sub>3</sub>O<sub>3</sub>, 1517.95; observed, 1517.65 (100.0%, M<sup>+</sup>).

**Compound 8.** <sup>1</sup>H NMR (300 MHz, CDCl<sub>3</sub>, 298 K):  $\delta$  = 8.16 (d, *J* = 5.4 Hz, 2H),  $\delta$  = 7.98 (m, 4H),  $\delta$  = 7.90 (d, *J* = 3 Hz, 2H),  $\delta$  = 3.79 (s, 2H),  $\delta$  = 3.26 (s, 2H); UV–vis (CH<sub>2</sub>Cl<sub>2</sub>):  $\lambda_{\max}(\epsilon)$  = 533 (228, 730), 644 (23930). MALDI-TOF MS *m/z*: Calcd for C<sub>66</sub>H<sub>12</sub>F<sub>30</sub>S<sub>3</sub>Se<sub>3</sub>, 1707.83; observed 1707.74 (100.0%, M<sup>+</sup>).

**Compound 9.** <sup>1</sup>H NMR (300 MHz, CDCl<sub>3</sub>, 298 K):  $\delta$  = 9.05 (d, *J* = 4.5 Hz, 4H),  $\delta$  = 9.17 (d, *J* = 4.5 Hz, 4H),  $\delta$  = –0.46 (s, 4H); UV–vis:  $\lambda_{\max}(\epsilon)$  = 551 (415600), 670 (38900), 726 (13650). MALDI-TOF MS *m/z*: Calcd for C<sub>66</sub>H<sub>12</sub>F<sub>30</sub>S<sub>6</sub>, 1565.8784; observed 1565.5331 (100.0%, M<sup>+</sup>).

**Synthetic procedure for 11, 12, and 13.** A similar procedure as mentioned above was followed with 2,5-(pentafluorophenylhydroxymethyl)thiophene, **6a**, 2,5-(pentafluorophenylhydroxymethyl) selenophene, **6b**, (0.5 mmol) and 2,2'-(pentafluorophenylmethylene)difuran, **10a**, 2,2'-(pentafluorophenylmethylene)dithiophene, **10b**, (0.5 mmol). Macrocycles **11**, **12**, and **13** were obtained in 11% (74 mg), 4% (32 mg), and 9% (82 mg), respectively.

**Compound 11.** <sup>1</sup>H NMR (300 MHz, CDCl<sub>3</sub>, 298 K):  $\delta$  = 9.07 (d, *J* = 4.2 Hz, 2H),  $\delta$  = 8.92 (d, *J* = 5.4 Hz, 2H),  $\delta$  = 8.63 (d, *J* = 4.5 Hz, 2H),  $\delta$  = 8.56 (d, *J* = 4.2 Hz, 2H),  $\delta$  = –0.17 (d, *J* = 4.5 Hz, 2H),  $\delta$  = –0.70 (d, *J* = 4.8 Hz, 2H); UV–vis (CH<sub>2</sub>Cl<sub>2</sub>):  $\lambda_{\max}(\epsilon)$  = 537(366800), 667(32300), 716(11050). MALDI-TOF MS *m/z*: Calcd for C<sub>66</sub>H<sub>12</sub>F<sub>30</sub>S<sub>2</sub>O<sub>4</sub>, 1501.97; observed, 1502.41 (100.0%, M<sup>+</sup>).

**Compound 12.** <sup>1</sup>H NMR (300 MHz, CDCl<sub>3</sub>, 298 K):  $\delta$  = 9.04 (d, *J* = 4.5 Hz, 2H),  $\delta$  = 8.93 (d, *J* = 5.4 Hz, 2H),  $\delta$  = 8.45 (d, *J* = 4.8 Hz, 2H),  $\delta$  = 8.40 (d, *J* = 4.8 Hz, 2H),  $\delta$  = 0.88 (d, *J* = 4.8 Hz, 2H),  $\delta$  = 0.41 (d, *J* = 4.8 Hz, 2H); UV–vis (CH<sub>2</sub>Cl<sub>2</sub>):  $\lambda_{\max}(\epsilon)$  = 542(392900), 667(36850), 726(16800). MALDI-TOF MS *m/z*: Calcd for C<sub>66</sub>H<sub>12</sub>F<sub>30</sub>Se<sub>2</sub>O<sub>4</sub>, 1596.67; observed, 1596.38 (100.0%, M<sup>+</sup>).

**Compound 13.** <sup>1</sup>H NMR (300 MHz, CDCl<sub>3</sub>, 298 K):  $\delta$  = 9.23 (d, *J* = 4.5 Hz, 4H),  $\delta$  = 9.13 (d, *J* = 4.5 Hz, 4H),  $\delta$  = –0.873 (s, 4H); UV–vis (CH<sub>2</sub>Cl<sub>2</sub>):  $\lambda_{\max}(\epsilon)$  = 557(433200), 675(45510).



MALDI-TOF MS  $m/z$ : Calcd for C<sub>66</sub>H<sub>12</sub>F<sub>30</sub>Se<sub>2</sub>S<sub>4</sub>, 1660.94; observed, 1661.08 (100.0%, M<sup>+</sup>).

**Single Crystal X-ray Diffraction Analysis.** Good quality single crystals were grown by slow evaporation of *n*-hexane into chloroform solutions of **7–9**, **11**, and **13**. The single crystal X-ray diffraction data were collected on a Bruker AXS Kappa Apex 2 CCD diffractometer, at 173(2) K for **7** and **9**, and 248(2) K for **8**, **11**, and **13**, equipped with graphite monochromated Mo(K $\alpha$ ) ( $\lambda = 0.7107$  Å) radiation and CCD detector. Crystals were cut to suitable size under nitrogen and immediately mounted on a glass fiber using cyanoacrylate adhesive. The structures were solved using the SIR92 program. The structures were refined using SHELXL-97 program. All the non-hydrogen atoms were refined with anisotropic displacement parameters. In all structures discussed in this thesis, most of the hydrogen atoms could be located in the difference Fourier map. However, the hydrogen

atoms whose positions could be assigned geometrically were constrained to those positions and were given riding model refinement.

**Acknowledgment.** The authors thank DST, New Delhi, India, for financial support and Dr. Babu Varghese, SAIF, IIT-Madras, Chennai, for single crystal X-ray diffraction data. J.S.R. thanks CSIR for a research fellowship.

**Supporting Information Available:** <sup>1</sup>H NMR, mass spectra, and CV data for all the macrocycles along with CIF for **7–9**, **11**, and **13**. This material is available free of charge via the Internet at <http://pubs.acs.org>.

JA906290D